

## Simplification of Gang Model of a Hybrid Photovoltaic Thermal System for Power Generation and Heat Conservation Using Phase Changing Materials

*Emeruwa, C.*

*Department of Physics, Federal University Otuoke, Nigeria*

### Article Info

*Article history:*

*Received 12 March 2021*

*Revised 20 March 2021*

*Accepted 27 March 2021*

*Available online 10 June 2021*

*Keywords:*

*Photovoltaic panel, pipes, phase change, evaporator, thermal conductivity, condenser*



<https://doi.org/10.37933/nipes.e/3.2.2021.7>

<https://nipesjournals.org.ng>

© 2021 NIPES Pub. All rights reserved

### Abstract

*This study designs a hybrid system which is made up of photovoltaic panels, heat pipes and phase changing materials for the purpose of power generation and heat conservation. A mathematical model was established to accurately determine the performance of the hybrid system. Through the model, the operating parameters such as the photovoltaic panel temperature, power output and waste heat could be determined for effective implementation.*

## 1. Introduction

Due to the environmental problems associated with fossil fuels, renewable energy is currently being used as a sustainable substitute for energy generation. Considering that the earth receives  $4.3 \times 10^{20}$  J of energy from sunlight in one hour [1], gives solar energy better potentials as compared to other forms of renewable energy. Solar energy is converted into electrical power directly through the use of photovoltaic (PV) cells. The conversion of solar energy to electrical power gives rise to heat as waste product. The production of heat accounts for the over 80% of solar energy not converted to electrical power by the photovoltaic cells [2]. The waste heat reduces the efficiency of the panels and thus the need to transfer the heat away from the panel. The most effective means of transferring this waste heat is by cooling. This process of cooling the PV panel gives rise to a hybrid Photovoltaic Thermal (PVT) system that generates electrical power and thermal energy for alternative use. The hybrid PVT system has the advantage of better performance because it offers a lower panel temperature during operation thus making it very competitive. For the purpose of cooling the panel, air or water coolant can be used but, in this work, water coolant is used due to the high thermal capacity and conductivity of water when compared to air.

This work focuses on developing a simplified mathematical model in line with Gang model for a hybrid photovoltaic thermal system that can be used to predict the performance of the system. Through this model, the electrical power generated and the temperatures of the associated

parameters such as water coolant, heat pipe evaporator and phase change material's melting point can be determined accurately.

### 1.1 System Description

The hybrid system is proposed to comprise of photovoltaic panels, heat pipe evaporators, water coolant/ phase changing materials (PCM) and water tank for storage. The PV panel's base is joined to the heat pipes by a thermally conductive layer while the opposite condenser end of the pipe is immersed in the tank containing the water coolant/ PCM. The proposed system is as shown in Figure 1. The PV panel is a standard panel with no intrinsic modifications, its better performance is as a result of the hybrid combination. The heat pipe is made of metal with capillary inner lining. It contains a small amount of coolant. Its function is to transfer the heat generated by the PV panel through the combined process of evaporation, vapor flow and condensation from the PV panel to the storage tank.

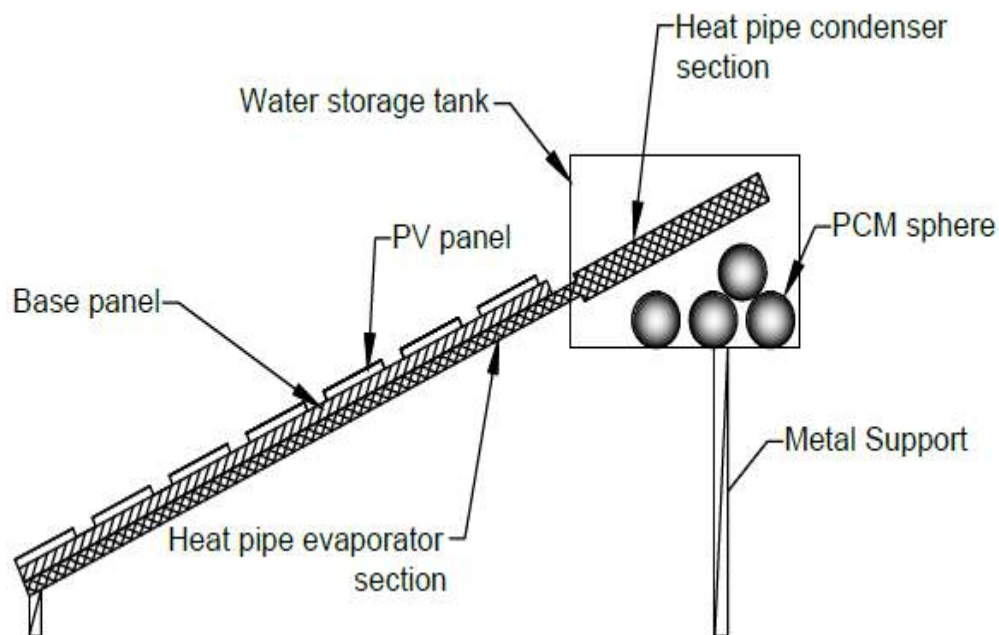


**Fig. 1: Schematic side view of the proposed system**

The coolant/PCM are heat storage materials placed inside the storage tank. Their function is to enhance the heat storage capacity of the tank. Their temperature rises as they absorb heat, this continues until their melting point is reached. Once the melting point is reached, the PCMs starts to melt without any visible change in temperature, thereby absorbing a greater amount of heat with no visible change in temperature [3, 4]. The PCM solidifies again whenever there is a drop in the surrounding water coolant temperature. Upon solidification, the PCM releases the stored thermal energy to the surrounding coolant.

### 1.2. Mathematical Simplification of the Model

Different formulations are used in developing the mathematical models for the different subsystems of the hybrid system. The formulation of Gang et al [5] is used for the mathematical model of the PV panel, heat pipe and base panel. Here, quasi-steady state operation is assumed within the various components of the system. The balanced energy equation considered in Gang model are the

Thermal-Balance Equation of the used PV panel, the Balanced Thermal Conduction in the base panel, the Thermal-Balances of the heat pipe and the Thermal-Balance for the water base coolant. In this simplified model, PCMs are introduced in the storage tank as part of the coolant. The introduction of PCM generates an additional energy balance equation in the storage tank.

In order to achieve these balance equations, two important assumptions are made and they are:

- (a) Considering that the thickness of the PV panel is much less than the width, the temperature variation along the thickness and base panel is assumed to be negligible.
- (b) Considering the uniformity of the operating temperature of the heat-pipe, the temperature variation of the PV panel and its base panel is assumed to be negligible in the heat pipe along the axial direction.

Using the Gang et al [5] numerical model, the thermal-balance equation for the PV panel is given as:

$$\delta_{pv}\rho_{pv}C_{pv}\frac{\partial T_{pv}}{\partial t} = h_a(T_a - T_{pv}) + h_{sky,pv}(T_{sky} - T_{pv}) + \frac{(T_b - T_{pv})}{R_{b,pv}} + \alpha_{pv}G - E_{pv} \quad (1a)$$

Where  $\delta_{pv}$  is the PV thickness

$\rho_{pv}$  is the PV density

$\alpha_{pv}$  is the PV absorptivity

$h_a$  is the convective heat transfer coefficient

$h_{sky,pv}$  is the radiant heat transfer coefficient

$T_{pv}$  is the PV panel temperature

$T_a$  is the base panel temperature

$T_{sky}$  is the sky temperature

Some of these parameters have constant values according to [6,7] as follows:

$$T_{sky} = 0.0552 T_a^{1.5}$$

$$h_a = 2.8 + U_a$$

$$h_{sky} = \varepsilon_{pv}\sigma(T_{sky}^2 + T_{pv}^2)(T_{sky} + T_{pv})$$

Where  $U_a$  is wind speed

$\varepsilon_{pv}$  is emissivity of the PV

$\sigma$  is Boltzman constant

The term  $R_{b,pv}$  represents the thermal contact resistance within the adhesive materials and it is expressed as

$$R_{b,pv} = \frac{\delta_{ad}}{K_{ad}}$$

Where  $\delta_{ad}$  is the adhesive material' thickness

$K_{ad}$  is the adhesive material' thermal conductivity

Following the formulations of [6], the electrical energy generated in the PV ( $E_{pv}$ ) is given as

$$E_{pv} = \gamma\alpha_{pv}G_{nr}[1 - B_r(T_{pv} - T_r)] \quad (1b)$$

Here  $\gamma$  is the coverage ratio of the PV cell

$G$  is the solar irradiation

$nr$  is the reference cell efficiency

$T_r$  is the operating reference temperature

$B_r$  is the temperature coefficient

Considering the basic assumptions and dividing the panel into two grids which is known as heat-pipe mode and fin plate. The one dimensional thermal-conduction equation was derived in line with [6,8] as

$$P_b C_b \frac{\partial T_b}{\partial t} = k_b \frac{\partial^2 T_b}{\partial x^2} + \frac{1}{\delta_b} \left[ \frac{(T_a - T_b)}{R_{b,a}} + \frac{(T_{pv} - T_b)}{R_{b,pv}} \right] \quad (2)$$

and

$$P_b C_b \frac{\partial T_b}{\partial t} = k_b \frac{\partial^2 T_b}{\partial x^2} + \frac{1}{\delta_b} \left[ \frac{(T_a - T_b)}{R_{b,a}} + \frac{(T_{pv} - T_b)}{R_{b,pv}} + \frac{(T_{p,evap} - T_b)}{R_{pb}} \right] \quad (3)$$

with all symbols having their usual meaning.

Within the evaporation section, it is assumed that evaporation occurs at a constant saturation pressure. Thus, the thermal-balance equation for the evaporator section and condenser according to the formulations of [9] are given as follows:

$$M_{p,evap} C_p \frac{\partial T_{p,evap}}{\partial T} = \frac{T_{p,cond} - T_{p,evap}}{R_{evap,cond}} + \frac{T_b - T_{p,evap}}{R_{p,b}} \quad (4)$$

$$M_{p,cond} C_p \frac{\partial T_{p,cond}}{\partial T} = \frac{T_{p,evap} - T_{p,cond}}{R_{evap,cond}} + A_{cond,w} h_{cond,w} (T_w - T_{p,cond}) \quad (5)$$

where  $M_{p,evap}$  is the mass of the evaporator

$M_{p,cond}$  is the mass of the condenser section of the heat pipe

$T_{p,cond}$  is the condenser temperature

$T_{p,evap}$  is the evaporator section temperature

$R_{evap,cond}$  is the sum thermal resistance of heat transfer from the evaporator section to the condenser section

$A_{cond,w}$  is the area of contact between the condenser section of the heat pipe and the coolant in the tank

$h_{cond,w}$  is the convection heat transfer coefficient

The sum thermal resistance  $R_{evap,cond}$  can be used to mathematically model the heat transfer from the evaporator to the condenser section within the heat pipe. The numerical value of  $R_{evap,cond}$  is derived as

$$R_{evap,cond} = R_{evap,wick} + R_{evap,i} + R_v + R_{cond,i} \quad (6)$$

Neglecting the thermal resistance in vapor flow direction according to [5, 9, 10], the thermal resistance across the wick thickness can be given as

$$R_{evap,wick} = \frac{\ln(D_{wick,o}/D_{wick,i})}{2\pi L_{evap} K_{wick}} \quad (7)$$

Here  $K_{wick}$  is the effective thermal conductivity of the saturated wick screen mesh structure used in the evaporation section of the heat pipe.

The value of  $K_{wick}$  can be calculated according to [9] as

$$K_{wick} = \frac{K_l [(K_l + K_s) - (1 - \xi_{wick})(K_l - K_s)]}{(K_l - K_s) + (1 - \xi_{wick})(K_l - K_s)} \quad (8)$$

Here  $K_l$  is the thermal conductivity of the working fluid

$K_s$  is the thermal conductivity of the wick material

$\xi_{wick}$  is the wick porosity

Now using the Azad formulation [11] the thermal resistance occurring at the vapor-liquid interfaces within the evaporator can be calculated as:

$$R_{evap,i} = \frac{2}{\pi D_{evap,i} L_{evap} h_{evap,i}} \quad (9a)$$

$$\text{where } h_{evap,i} = \frac{K_l}{t_{wick}} \quad (9b)$$

but the thermal resistance associated with the condensing process is given as

$$R_{cond,i} = \frac{1}{\pi D_{cond,i} L_{cond} h_{cond,i}} \quad (9c)$$

Where  $h_{cond,i}$  is the condensing film coefficient and is expressed mathematically as

$$h_{cond,i} = 1.13 \left[ \frac{g \sin \theta \cdot \rho_l (\rho_l - \rho_v) K_l^3 h_{fg}}{\mu_l \Delta T_{cr} L_{cond}} \right]^{1/4} \quad (9d)$$

Where  $\rho_l$  is the liquid density of the working fluid

$\rho_v$  is the vapor density of the working fluid

$\Delta T_{cr}$  is the critical temperature difference

$$\Delta T_{cr} = |T_{cond,i} - T_l|$$

The formulation of Hussein et al [12] is used in calculating the working fluid saturation temperature ( $T_l$ ) and the calculation assumes relative constant temperature in the storage tank due to the presence of PCMs and that the working fluid in the heat pipe is wholly saturated:

$$\frac{\pi}{4} D_{evap,i}^2 L_{evap} \rho_l C_l R_v^* \frac{\partial T_l}{\partial t} = \pi D_{evap,i} L_{evap} h_{evap,i} (T_{p,evap} - T_l) - \pi D_{cond,i} L_{cond} h_{cond,i} (T_l - T_{p,cond}) \quad (10)$$

Here  $R_v^*$  is the liquid filling ration

There is also need to balance energy within the storage tank and in doing this, the sensible and latent heat are considered. The tank is divided into control volumes to correspond to the condenser section of the heat pipe and each control volume contains equal amount of a phase changing material. Assuming that the temperature of each control volume is uniform, the heat-balance equation for the coolant (water) and PCM in the control volume of the tank is expressed as:

$$\rho_w V_w C_w \frac{\partial T_w}{\partial t} = \frac{T_a - T_w}{R_{a,w}} + A_{cond,w} h_{cond,w} (T_{p,cond} - T_w) + n_{pcm} h_{w,pcm} A_{pcm} (T_{pcm} - T_w) \quad (11a)$$

Heat loss to the atmosphere is represented by the first term on the right side of the equation, the middle term represents the convection heat transfer while the last term represent the sensible heat transfer between the PCM and water.

The term  $h_{w,pcm}$  is the free convection heat transfer and is expressed as

$$h_{w,pcm} = \frac{N \mu_{w,pcm} \times K_w}{D_{pcm,o}} \quad (11b)$$

By the help of Incropera et al [13] the Nusselt number is determined using the formula

$$N \mu_{w,pcm} = 2 + \frac{0.589 R_Y^{1/4}}{[1 + (0.469 / Pr_w)^{9/16}]^{4/9}} \quad (12a)$$

where  $Pr_w$  is the Prandtl number

$R_Y$  is the Rayleigh number

The Rayleigh number is further expressed as

$$R_Y = \frac{g B_w (T_{pcm} - T_w) D_{pcm}^3}{V_w \alpha_w} \quad (12b)$$

where  $\alpha_w$  is the thermal diffusivity of water

Neglecting the natural convection and thermal resistance of the PCM, the thermal energy balance equation for the PCM during sensible heating is expressed mathematically as

$$M_{pcm} C_{pcm} \frac{\partial T_{pcm}}{\partial t} = \frac{(T - T_{pcm})}{R_{w,pcm}} \quad (13a)$$

here  $M_{pcm}$  is the mass of each PCM sphere

$R_{w,pcm}$  is the thermal resistance between water and the PCM

$$R_{w,pcm} = \frac{1}{h_{w,pcm} A_{pcm}} \quad (13b)$$

The PCM melts when the temperature reaches their melting point, this melting process is accompanied by a gain or loss of heat depending on weather there is melting or freezing. At the point of melting, the thermal balance equation is given as

$$M_{pcm} h_{melting} = \frac{\partial K_{liquid}}{\partial t} = \frac{(T_w - T_{pcm})}{R_{w,pcm}} \quad (14)$$

here  $h_{melting}$  is the latent heat of fusion while  $K_{liquid}$  is the liquid fraction of the PCM.

### 1.3. Maple Simulation

The balance energy equations are quantized both in time and space for the corresponding hybrid panel. Each heat pipe evaporator section is divided to identical elements with corresponding fin plate which represents one element in the lateral direction. The quantization did not extend to the axial direction as the parameters therefore they are considered negligible due to the uniformity of the operating temperature in that direction. The quantized balance energy equations are given as follows and are employed in calculating the values of the panel's heat pipe's water and PCM's temperatures respectively.

For standard PV panel

$$\delta_{pv}\rho_{pv}C_{pv}\frac{T_{pv,i'}-T_{pv,i}^0}{\Delta t} = h_a(T_a - T_{pv,i'}) + h_{sky,pv}(T_{sky} - T_{pv,i'}) + \frac{T_{b,i'}}{R_{b,pv}} + \alpha_{pv}G - E_{pv} \quad (15)$$

For the base panel middle node

$$\rho_b C_b \frac{T_{b,i'}-T_{b,i}^0}{\Delta t} = X_b \frac{T_{b,i'}-2T_{b,i'}+T_{b,i-1}'}{\Delta x^2} + \frac{1}{\delta_b} \left[ \frac{(T_a-T_{b,i'})}{R_{b,a}} + \frac{(T_{pv,i'}-T_{b,i'})}{R_{b,pv}} \right] \quad (16)$$

For the base panel heat pipe node

$$\rho_b C_b \frac{T_{b,i'}-T_{b,i}^0}{\Delta t} = X_b \frac{T_{b,i'}-2T_{b,i'}+T_{b,i-1}'}{\Delta x^2} + \frac{1}{\delta_b} \left[ \frac{(T_a-T_{b,i'})}{R_{b,a}} + \frac{(T_{pv,i'}-T_{b,i'})}{R_{b,pv}} + \frac{(T_{p,evap,i'}-T_{b,i'})}{R_{p,b}} \right] \quad (17)$$

For heat pipe evaporator section

$$M_{p,evap}C_p \frac{T_{p,evap,i'}-T_{p,evap,i}^0}{\Delta t} = \frac{T_{p,cond,i'}-T_{p,evap,i'}}{R_{evap,cond}} + \frac{T_{b,i'}-T_{p,evap,i'}}{R_{p,b}} \quad (18)$$

For heat pipe condenser section

$$M_{p,cond}C_p \frac{T_{p,cond,i'}-T_{p,cond,i}^0}{\Delta t} = \frac{T_{p,evap,i'}-T_{p,cond,i'}}{R_{evap,cond}} + A_{cond,w}h_{cond,w}(T_{w,i'} - T_{p,cond,i'}) \quad (19)$$

For storage tank containing water and PCM

$$\rho_w V_w C_w \frac{T_{w,i'}-T_{w,i}^0}{\Delta t} = \frac{T_a-T_{w,i'}}{R_{a,w}} + A_{cond,w}h_{cond,w}(T_{p,cond,i'} - T_{w,i'}) + n_{pcm}h_{w,pcm}A_{pcm}(T_{pcm,i'} - T_{w,i'}) \quad (20)$$

$$M_{pcm}C_{pcm} \frac{T_{pcm,i'}-T_{pcm,i}^0}{\Delta t} = \frac{(T_{w,i'}-T_{pcm,i'})}{R_{w,pcm}} \quad (21)$$

$$M_{pcm}h_{melting} \frac{x_{liquid}'-x_{liquid}^0}{\Delta t} = \frac{(T_{w,i'}-T_{pcm,i'})}{R_{w,pcm}} \quad (22)$$

## 2.0 Results and Validation

The physical and geometric parameters of system components and average typical weather and solar data were used as input for the simplified model simulation. The simulation starts from a near uniform PCM and water temperatures of 25.2C. The PVT panel and Standard PV panel initial temperatures were set at 25.1C and 24.4C respectively. These initial temperatures served as simulation input for the first hour. The model's predictions are compared with the experimentally measured values of temperatures of PVT panel, Standard PV panel and water according to Abed [14] Figure 3 shows the model prediction for a hybrid PVT panel and a standard PVT panel. For both cases, there was a rise in temperature starting from the early stage until it reaches peak while corresponds to around mid-day. After the peak is reached, the temperature drops gradually for the

rest of the simulation. The maximum temperature attained for the panel surface for the hybrid PVT panel surface is 49.6°C while the standard PV panel surface temperature maximum reached 64.74°C, this clearly show a temperature drop of 15.14°C at peak hour between the standard PV and hybrid PVT panel.

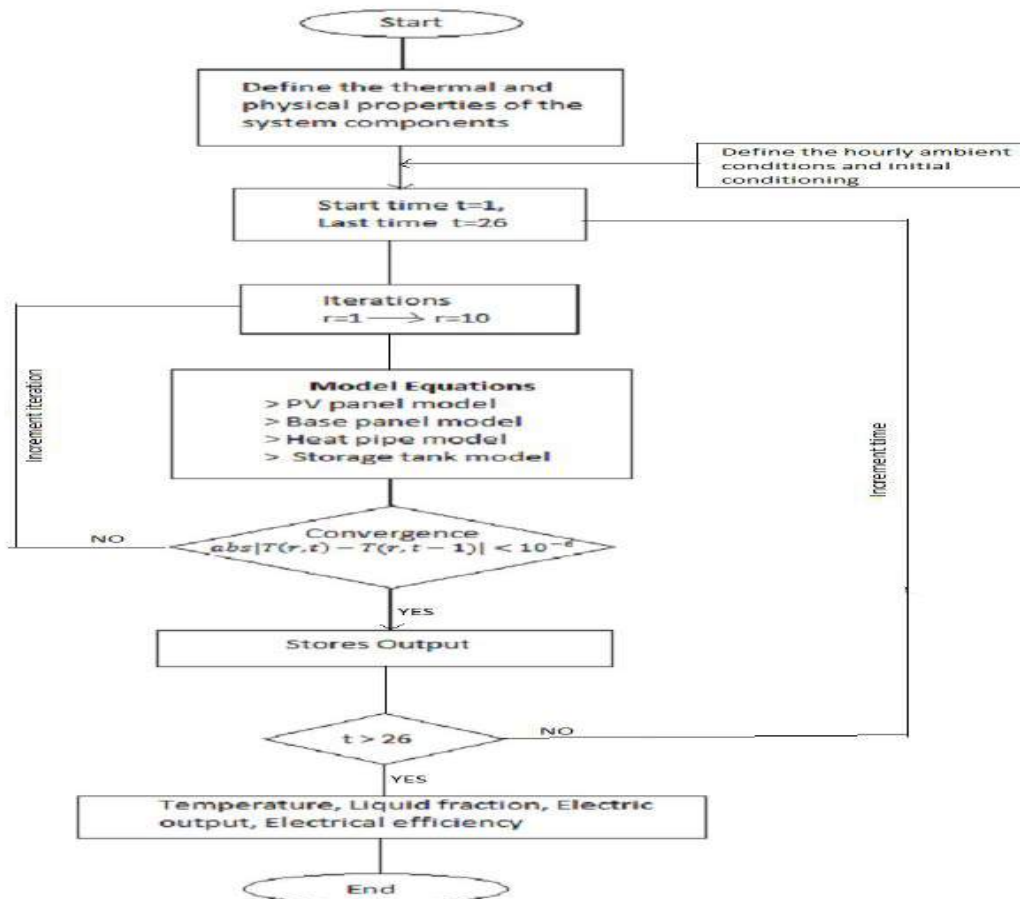


**Fig 2: Flow chart of simulation**

Figure 4 shows the variation of water temperature in the storage tank. It is seen that the temperature of the water increased as the solar irradiance increased until the PCM starts to melt at around 28°C. The water temperature stabilizes at a nearly constant temperature while the PCM melts completely thereby changing phase from solid to liquid. The PCM thus maintains a nearly constant water temperature thus functioning as a suitable heat sink for the heat pipe’s condenser of the hybrid PVT system. When the PCM melts completely, a sensible increase in the water temperature is further observed.

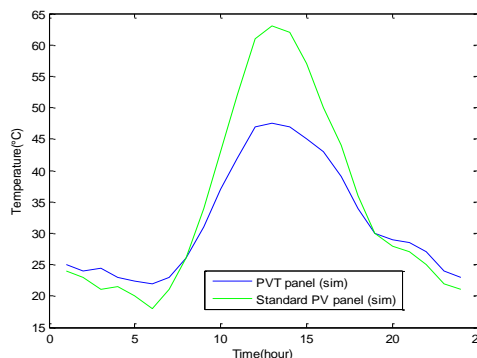


**Fig.3: Plot of the PV panel temperature for Standard PV panel and Hybrid PVT panel**

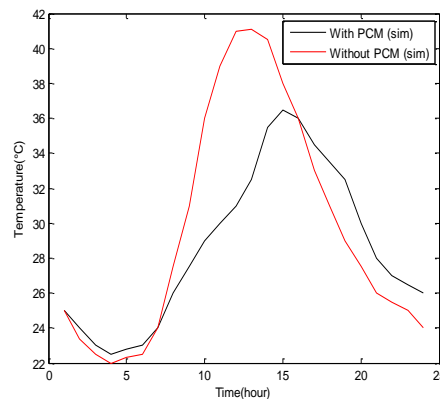


**Fig.4: Variation of the storage tank temperature with PCM and without PCM**

### 3.0 Conclusion

The possibility of implementing a simplified version of Gang model of a hybrid PVT system has been evaluated by adding a Phase Changing Material to the system which enables the storage tank temperature to remain constant while the different components are integrated to form the hybrid system. The model was found to be effective in providing a maximum reduction of 15.14°C in the operating temperature of PV panel during operation which translates directly to an increase in the electrical power output. The electrical efficiency was also found to have improved by about 10%.

### References

- [1] Zondag, H.A.(2008) Flat-plate PV-Thermal collectors and systems: A review. *Renewable and Sustainable Energy Reviews*;12(4): 891–959.
- [2] Kumar, R and Rosen M.A.(2011) A critical review of photovoltaic-thermal solar collectors for air heating. *Applied Energy*; 88(11): 3603–3614.
- [3] Garg, H.P and Adhikari, R.S.(1999) Performance analysis of a hybrid photovoltaic/thermal (PV/T) collector with integrated CPC troughs. *International Journal of Energy Research*; 23(15):1295-1304.
- [4] Kumar, R. and Rosen, M.A.(2011) Performance evaluation of a double pass PV/T solar air heater with and without fin. *Applied Thermal Engineering*; 31(8):1402–1410.
- [5] Gang, P., Huide, F., Tao, Z. and Jie, J.(2011) A numerical and experimental study on a heat pipe PV/T system. *Solar Energy*; 85(5): 911–921.
- [6] Tonui, J.K. and Tripanagnostopoulos, Y. (2007) Improved PV/T solar collectors with heat extraction by forced or natural air circulation. *Renewable Energy*; 32(4):623-637.
- [7] Kalogirou, S.A. (2001) Use of TRNSYS for modelling and simulation of a hybrid pv–thermal solar system for Cyprus. *Renewable Energy*; 23(2):247–260.
- [8] Krauter, S. (2004) Increased electrical yield via water flow over the front of photovoltaic panels. *Solar Energy Materials and Solar Cells*; 82(1-2):131–137.
- [9] Abdolzadeh, M. and Ameri, M. (2009) Improving the effectiveness of a photovoltaic water pumping system by spraying water over the front of photovoltaic cells. *Renewable Energy*; 34(1): 91–96.
- [10] Wu, S.Y., Zhang, Q.L., Xiao, L. and Guo, F.H. (2011) A heat pipe photovoltaic/thermal (PV/T) hybrid system and its performance evaluation. *Energy and Buildings*; 43(12): 3558–3567.
- [11] Azad, E. (2008) Theoretical and experimental investigation of heat pipe solar collector. *Experimental Thermal and Fluid Science*; 32(8): 1666-1672.
- [12] Hussein, H.M.S., Mohamad, M.A. and El-Asfour, A.S. (1999) Optimization of a wickless heat pipe flat plate solar collector. *Energy Conversion and Management*; 40(18): 1949-1961.
- [13] Incropera, F.P., Dewitt, D.P., Bergman, T.L. and Lavine, A.S. (2007) *Fundamentals of heat and mass transfer*, 6th ed. USA: John Wiley & Sons.
- [14] Abed, E. H. (2015) Optimized Design and Operation of Heat-Pipe PV/T System. *IOSR Journal of Electronics and Communication Engineering*, Volume 9, Issue 2, Pp 111-121.